Electronic Supplementary information (ESI)

For

Solvent-shielding allows the self-assembly of supramolecular 1D barium vanadate chains

Katharina Kastner[a] and Carsten Streb[a,b]*

[a]Department Chemistry and Pharmacy, Institute of Inorganic Chemistry II, Friedrich-Alexander-University Erlangen-Nuremberg, Egerlandstr. 1, 91058 Erlangen, Germany
[b]Ulm University, Institute of Inorganic Chemistry I, Albert-Einstein-Allee 11, 89081 Ulm, Germany
*Email: carsten.streb@chemie.uni-erlangen.de; carsten.streb@uni-ulm.de

1. Instrumentation

X-ray diffraction: Single-crystal X-ray diffraction studies were performed on a Nonius Kappa CCD Single-crystal X-ray diffractometer equipped with a graphite monochromator using MoKα radiation (wavelength λ(Mo-K_α) = 0.71073Å).

UV-Vis spectroscopy: UV-Vis spectroscopy was performed on a Shimadzu UV-2401PC spectrophotometer, Varian Cary 50 spectrophotometer or Varian Cary 5G spectrophotometer equipped with a Peltier thermostat. All systems were used with standard cuvettes (d = 10.0 mm).

Diffuse reflectance UV-Vis spectra were recorded on a Jasco V650 spectrophotometer. Samples were referenced against $BaSO_4$.

Thermogravimetric analysis (TGA): TGA was performed on a Setaram Setsys CS Evo, 30-1000℃ @ 10K/min, 200 mL/min He, Graphite c rucible 0.5 mL.

Atomic absorption spectroscopy: Atomic absorption spectroscopy analysis was performed on a Perkin Elmer 5100 PC spectrometer.

FT-IR spectroscopy: FT-IR spectroscopy was performed on a Shimadzu - FT-IR Prestige-21 spectrometer including a Golden Gate-ATR-unit. Signals are given as wavenumbers in cm^{-1} using the following abbreviations: vs = very strong, s = strong, m = medium, w = weak and b = broad.

Elemental analysis: Elemental analysis was performed on a Euro Vector Euro EA 3000 Elemental Analyzer.

General remarks: All chemicals were purchased from Sigma Aldrich, ACROS or ABCR and were of reagent grade. The chemicals were used without further purification unless stated otherwise.

Mass spectrometry (MS):

MS measurements were performed on a UHR-TOF Bruker Daltonik (Bremen, Germany) maXis, an ESI-ToF MS capable of resolution of at least 40,000 FWHM. Detection was in negative-ion mode and the source voltage was 4 kV. The flow rates were 500 µL/hour. The drying gas (N_2), to aid solvent removal, was held at 180 °C. The machine was calibrated prior to every experiment via direct infusion of the Agilent ESI-TOF low concentration tuning mixture, which provided an m/z range of singly charged peaks up to 2700 Da.

CSI-MS measurements were performed on a UHR-TOF Bruker Daltonik (Bremen, Germany) maXis, which was coupled to a Bruker cryospray unit, an ESI-ToF MS capable of resolution of at least 40,000 FWHM. Detection was in negative-ion mode and the source voltage was 4.5 kV (for compound 1) and 2.5 kV (for compound 2), respectively. The flow rates were 300 µL/hour. The drying gas (N_2), to aid solvent removal, was held at -35 °C and the spray gas was held at -40 °C. The machine was calibrated prior to every experiment via direct infusion of the Agilent ESI-TOF low concentration tuning mixture, which provided an m/z range of singly charged peaks up to 2700 Da in both ion modes.

2. Synthetic section

2.1 Synthesis of (^{n}BuN)$_2$[H$_4$V$_{10}$O$_{28}$]

V_2O_5 (16 g, 86.87 mmol) were suspended in water (100 mL) and the pH was adjusted to 12.5 with a saturated aqueous solution of NaOH. Then the pH was slowly decreased by dropwise addition of HCl (6 M) to pH 3.0. The reaction mixture turned from slightly orange to reddish orange. The reaction mixture was added dropwise to a solution of (^{n}Bu$_4$N)Br (17 g, 52.74 mmol) in water (100 mL). The orange precipitate was filtered off, washed with water, ethanol and Et_2O and dried.

Yield: 22.5 g (15.56 mmol, 88 % of crude product based on V).

Elemental analysis for $C_{32}H_{76}N_2V_{10}O_{28}$ in wt.-% (calcd.): C 26.45 (26.57), H 5.43 (5.30), N 1.89 (1.94).

2.2 Synthesis of {[Ba(nmp)$_4$(H$_2$O)]$_2$[H$_4$V$_{10}$O$_{28}$]}{[Ba(nmp)$_3$(H$_2$O)$_2$][H$_3$V$_{10}$O$_{28}$]}$_2$ x 2H$_2$O x 10 NMP}$_\infty$ (Compound 1)

$BaBr_2$ x $2H_2O$ (157 mg, 0.474 mmol, 1.7 eq) and 400 mg (^{n}Bu$_4$N)$_2$[H$_4$V$_{10}$O$_{28}$] (400 mg, 0.277 mmol, 1 eq) were suspended in 10 mL *N*-Methyl-2-pyrrolidone and 500µL water. The reaction mixture was heated up to 70 ℃ until it turned into a clear, orange solution. Diffusion crystallisation with acetone as diffusion solvent resulted in yellow plate crystals.

Yield: 450 mg (0.076 µmol, 82 % of crude product based on V).

Elemental analysis for $Ba_4C_{120}H_{242}N_{24}V_{30}O_{116}$ in wt.-% (calcd.): C 24.78 (24.20), H 3.74 (4.09), N 5.40 (5.65), Ba 8.44 (9.22), V: 24.94 (25.66).

Characteristic IR bands (in cm^{-1}): 3151 (b), 2957(w), 2929 (w), 2875 (w), 1628 (s), 1508 (m), 1476 (w), 1456 (w), 1447/1444 (w), 1425 (w), 1405 (m), 1309 (m), 1260 (m), 1178 (w), 1120 (m), 985/972/960/945 (s), 827 (s), 752 (m), 720 (m), 659 (w).

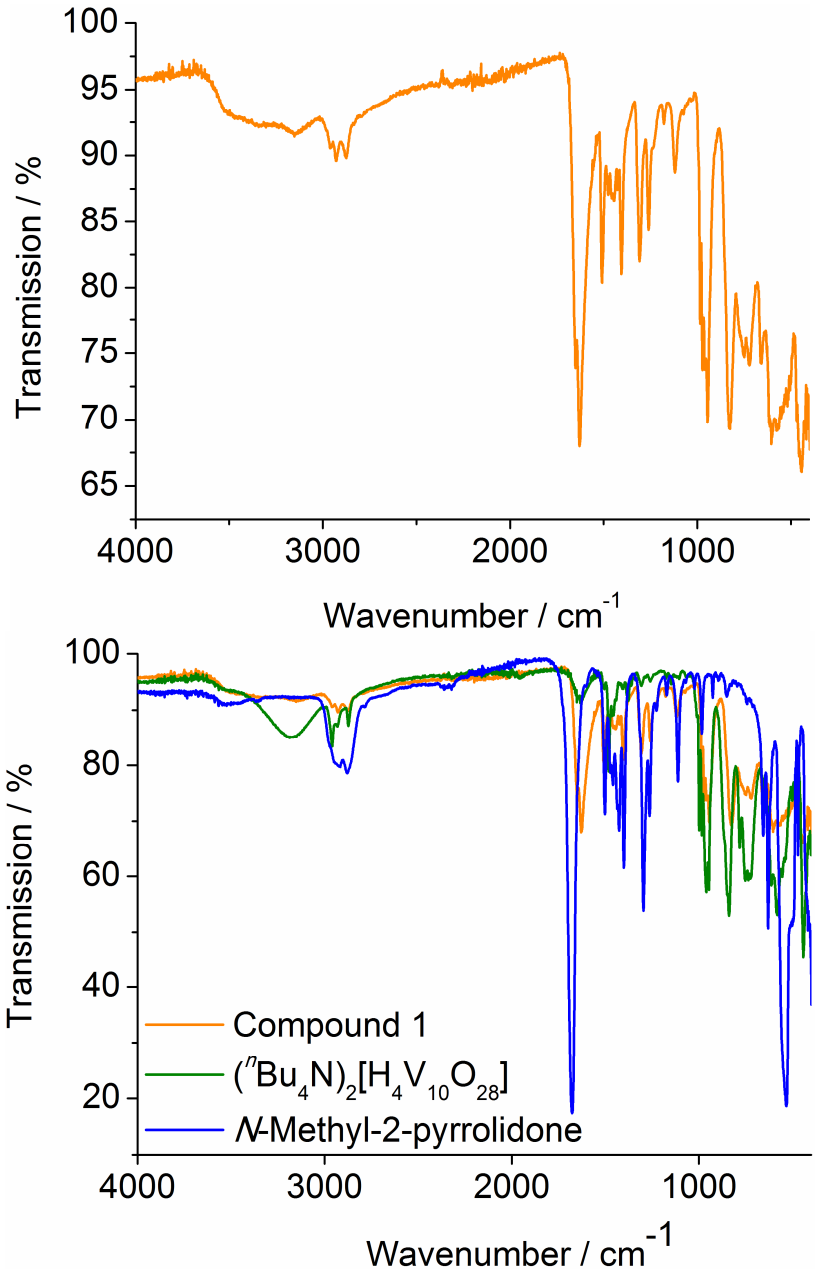

Figure S 1 Top: FT-IR spectrum of {[Ba(nmp)$_4$(H$_2$O)]$_2$[H$_4$V$_{10}$O$_{28}$]} {[Ba(nmp)$_3$(H$_2$O)$_2$][H$_2$V$_{10}$O$_{28}$]}$_2$ x 2 H$_2$O x 10 NMP}$_\infty$ showing the characteristic V-O vibrational modes in the fingerprint region < 1000 cm^{-1} and solvent molecule based stretching modes. **Bottom:** Comparison of FT-IR spectra of [Ba$_2$(nmp)$_8$(H$_2$O)$_2$(H$_3$V$_{10}$O$_{28}$)$_2$) (Ba$_2$(nmp)$_6$(H$_2$O)$_4$(H$_4$V$_{10}$O$_{28}$))], the precursor (^{n}Bu$_4$N)$_2$[H$_4$V$_{10}$O$_{28}$] and the solvent *N*-Methyl-2-pyrrolidone.

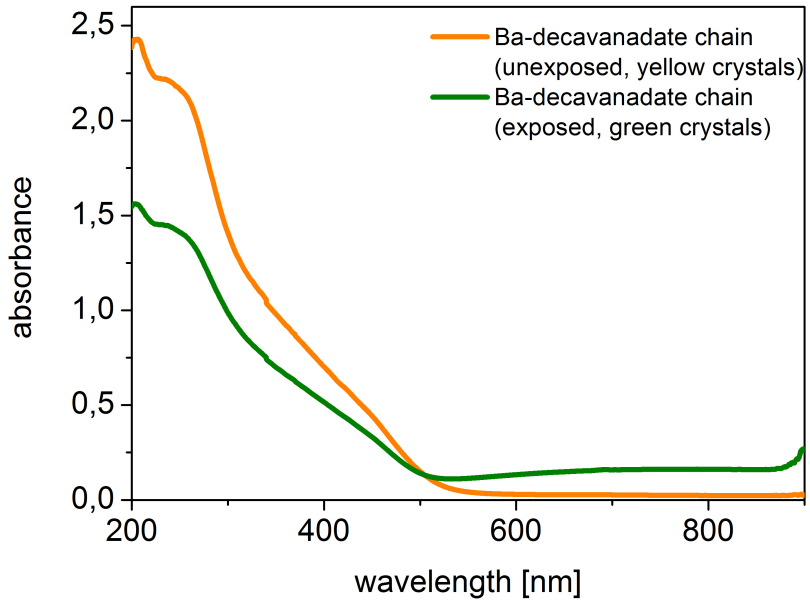

Figure S 2 UV-Vis spectra of compound **1** (orange) and compound **1** after irradiation with visible light for 24 h (green). The spectral changes indicate a solid-state redox reaction, most likely between the vanadium centres (reduction) and the NMP ligands (oxidation).

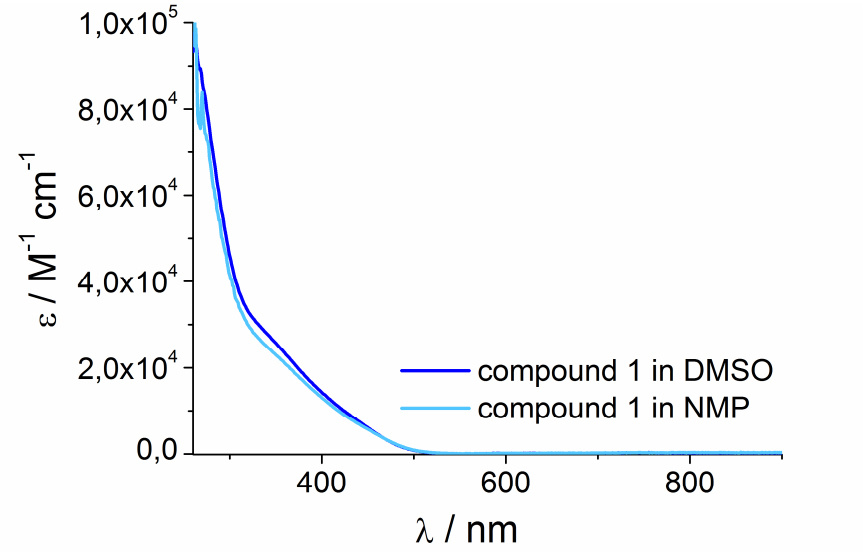

Figure S 3 UV-Vis spectra of compound **1** dissolved in DMSO (dark blue) and NMP (bright blue).

2.3 Synthesis of $\{[Ba(dmf)_4]_2[H_2V_{10}O_{28}]\}_\infty$ (Compound 2)

Compound **1** (100 mg, 0.017 mmol) was dissolved in 8 mL *N*-*N*-dimethyl formamide (DMF) and was stirred at room temperature for 4 h. Diffusion crystallisation with acetone as diffusion solvent resulted in yellow blocks.

Yield: 45 mg (0.025 µmol, 49 % of crude product based on V).

Elemental analysis for for $Ba_2C_{24}H_{58}N_8V_{10}O_{36}$ in wt.-% (calcd.): C 15.29 (15.85), H 3.10 (3.21), N 6.11 (6.16), Ba 14.86 (15.10), V: 28.23 (28.00).

Characteristic IR bands (in cm^{-1}): 3528 (b), 3372 (b), 2929 (w), 2880 (w), 2810 (w), 2160 (w), 2031 (w), 1672 (m), 1641 (s), 1597 (m), 1497 (m), 1435 (m), 1414 (m), 1387 (m), 1250 (w), 1152 (w), 1101 (m), 1067 (w), 970/953/943 (s), 826 (s), 746 (m), 664 (m).

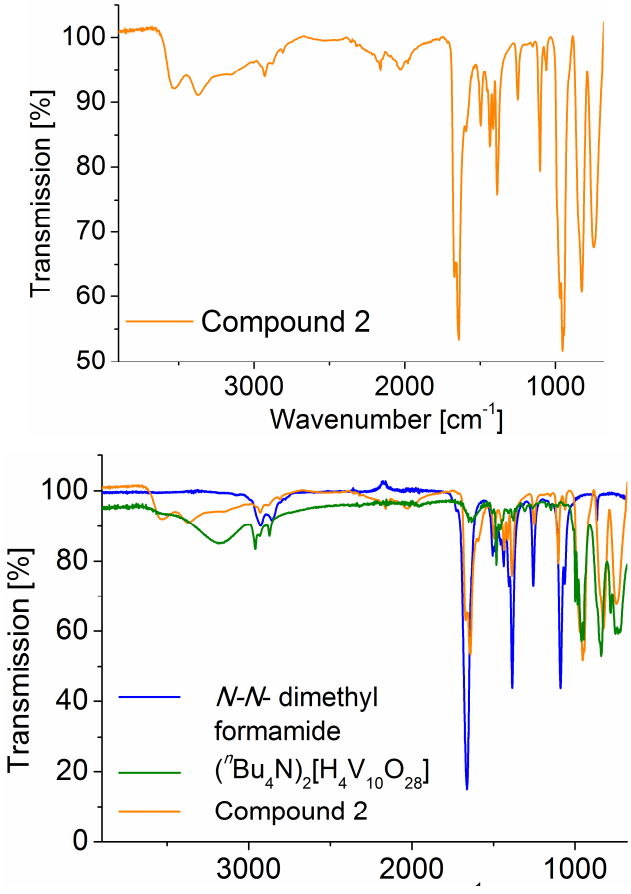

Figure S 4 Top: IR spectrum of $\{[(Ba(dmf)_4]_2[H_2V_{10}O_{28}]\}_\infty$ (Compound 2) showing the characteristic V-O vibrational modes in the fingerprint region < 1000 cm^{-1} and solvent molecule based stretching modes. **Bottom:** Comparison of FT-IR spectra of $\{[(Ba(dmf)_4]_2[H_2V_{10}O_{28}]\}_\infty$, the precursor $(^nBu_4N)_2[H_4V_{10}O_{28}]$ and the solvent *N*-*N*-dimethyl formamide.

3. Crystallographic information

Single-Crystal Structure Determination: Suitable single crystals of the respective compound were grown and mounted onto the end of a thin glass fiber using Fomblin oil. X-ray diffraction intensity data were measured at 150 K on a Nonius Kappa CCD diffractometer [λ(Mo-K_α) = 0.71073 Å] equipped with a graphite monochromator. Structure solution and refinement was carried out using the SHELX-97 package[S1] *via* WinGX.[S2] Corrections for incident and diffracted beam absorption effects were applied using empirical methods.[S3] Structures were solved by a combination of direct methods and difference Fourier syntheses and refined against F^2 by the full-matrix least-squares technique. Crystal data, data collection parameters and refinement statistics are listed in Table S1. These data can be obtained free of charge via www.ccdc.cam.ac.uk/conts/retrieving.html or from the Cambridge Crystallographic Data Center, 12, Union Road, Cambridge CB2 1EZ; fax:(+44) 1223-336-033; or deposit@ccdc.cam.ac.uk. CCDC reference numbers 928366 (**1**) and 928367 (**2**).

Table S 1 Crystallographic data for **1** and **2**

	Compound **1**	Compound **2**
Formula	$C_{55}H_{92}Ba_2N_{11}O_{57}V_{15}$	$C_{24}H_{54}Ba_2N_8O_{36}V_{10}$
M_r [g mol^{-1}]	2854.65	1814.83
Crystal system	Triclinic	Triclinic
Space group	*P*-1	*P*-1
a [Å]	12.240(2)	11.340(2)
b [Å]	13.285(3)	11.638(2)
c [Å]	33.139(7)	12.492(3)
α [°]	98.09(3)	104.74(3)
β [°]	91.58(3)	103.04(3)
γ [°]	106.32(3)	107.93(3)
ρ_{calcd} [g cm^{-3}]	1.856	2.105
V [Å]	5107(2)	1431.8(5)

Z	2	1
$\mu(Mo_{K\alpha})$ [μm^{-1}]	2.156	2.999
T [K]	150	150
F(000)	2817	884
min, max θ [°]	5.82, 26.50	5.80, 26.37
no refls measured	116359	34583
no refls unique	14582	4323
no parameters	1343	436
GooF	1.054	1.030
*R*1 (I > 2σ(I))	0.0570	0.0503
*wR*2 (all data)	0.1411	0.1261
max/min resd /e Å^{-3}	0.988 / -1.586	0.988 / -1.157

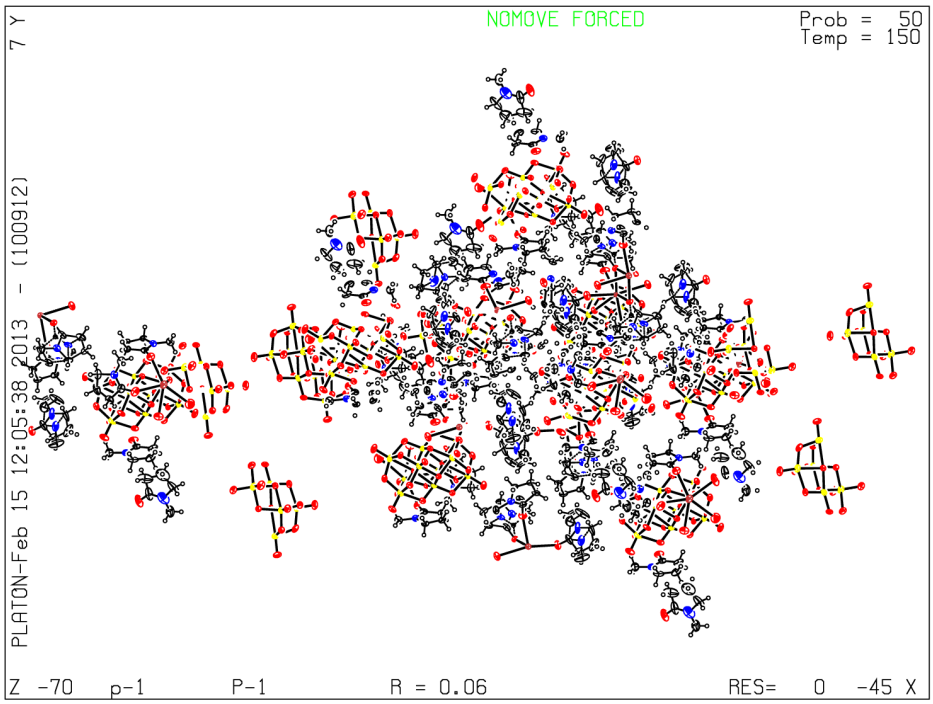

Figure S 4: ORTEP-plot of compound **1**, probability ellipsoids given at 50 %. Several NMP ligands were disordered over two positions. The structure was refined to satisfactory R values.

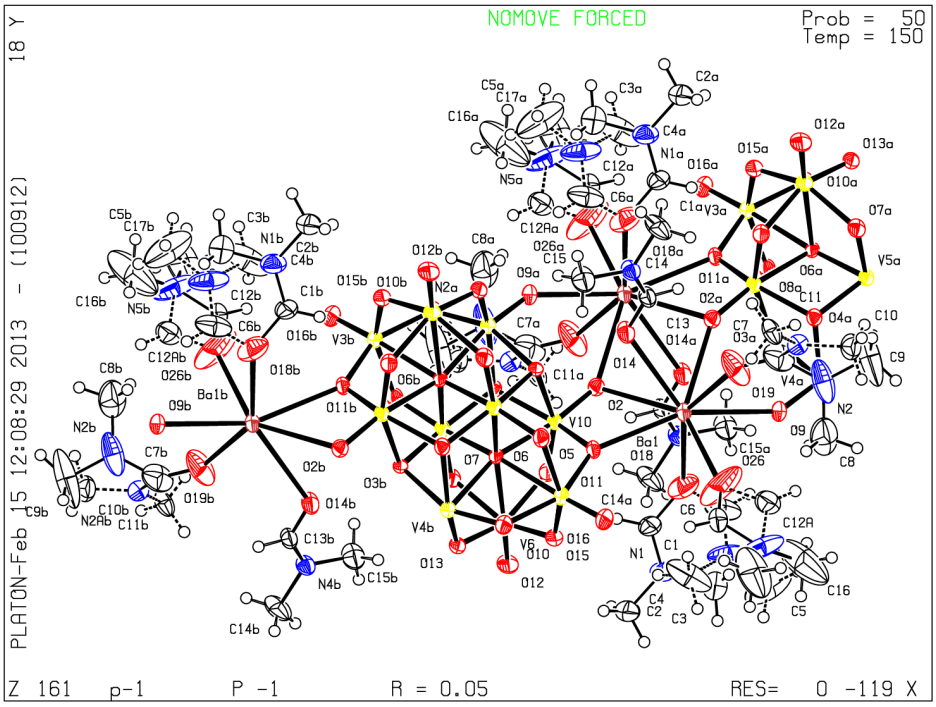

Figure S 5: ORTEP-plot of compound **2**, probability ellipsoids given at 50 %. Several DMF ligands were modeled using a disorder over two positions. This allowed refinement of the structure to satisfactory R values.

BVS-Calculations for compound 1:

Characterization of the protonation of the oxygen atoms of the vanadate clusters using bond valence sum calculations of compound **1** indicated that the oxygen atoms O30 (BVS 1.334) and O35 (BVS 1.344) are mono-protonated. Both oxygen ligands feature two symmetry-related positions in the decavanadate cluster, giving an overall fourfold cluster protonation $[H_4V_{10}O_{28}]^{2-}$.

Bond valence sum calculations also indicate that the oxygen atoms O4 (BVS- 1.247), O15 (BVS 1.186) and O22 (BVS 1.135) located on the second decavanadate cluster are mono-protonated, giving $[H_3V_{10}O_{28}]^{3-}$.

BVS-Calculations for compound 2:

Characterization of the protonation of the oxygen atoms of the vanadate clusters using bond valence sum calculations of compound **2** indicated that oxygen atom O3 (BVS

1.281) is mono-protonated. O3 features two symmetry-related positions, giving an overall di-protonated cluster species $[H_2V_{10}O_{28}]^{4-}$.

All oxygen atoms identified by BVS as being protonated also feature short intermolecular contacts to hydrogen-bond acceptors (NMP, H_2O), thus further substantiating the protonation assignment.

4. Mass spectrometry

4.1 ESI-MS measurements were performed on {[Ba(nmp)$_4$(H$_2$O)]$_2$[H$_4$V$_{10}$O$_{28}$]} {[Ba(nmp)$_3$(H$_2$O)$_2$][H$_2$V$_{10}$O$_{28}$]}$_2$ x 2H$_2$O x 10 NMP}$_\infty$ (*ca*. 1 x 10^{-4} M in DMF/MeCN (1:4, v:v)) in negative (-ve) ion mode.

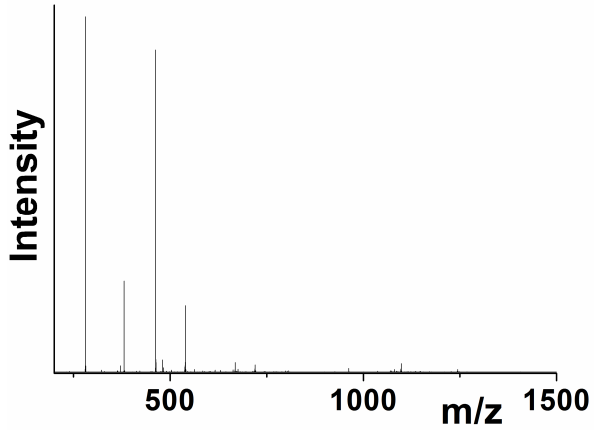

Figure S 5 Negative mode high resolution ESI mass spectrum of compound **1** ca. 1 x 10^{-5} M in DMF/MeCN (1:4, v:v).

Table S 2 Peak assignments for ESI-MS Spectrum of compound **1** in DMF/MeCN (1:4, v:v).

recorded m/z	calculated m/z	peak assignment
280.78	280.790	$[V_6O_{16}]^{2-}$
380.72	380.73	$H[V_4O_{11}]^{1-\ S4}$
462.64	462.65	$[V_{10}O_{26}]^{2-\ S4}$
468.65	468.66	$H_4[V_{10}O_{28}]^{2-}$
539.59	539.60	$[BaV_{10}O_{27}]^{2-}$
662.83	662.84	$[Ba(V_{10}O_{26})_2]^{3-}$
668.50	668.51	$H[Ba(V_{10}O_{26})(V_{10}O_{27})]^{3-}$
714.13	714.14	$Ba_2[(V_{10}O_{26})(V_{10}O_{27})]^{3-}$
719.79	719.81	$HBa_2[(V_{10}O_{27})_2]^{3-}$
766.92	766.93	$Ba_2[(V_{10}O_{26})_2(V_{10}O_{27})]^{4-}$
805.39	805.41	$Ba_3[(V_{10}O_{26})(V_{10}O_{27})_2]^{4-}$
1086.20	1086.22	$[H_5Ba_3(V_{10}O_{27})_2(V_{10}O_{28})]^{3-}$
1098.20	1098.23	$H_6Ba_2[(V_{10}O_{28})_2]^{2-}$

4.2 ESI-MS measurements were performed on **compound** 1 (*ca*. 1 x 10^{-4} M in MeOH) in negative (-ve) ion mode.

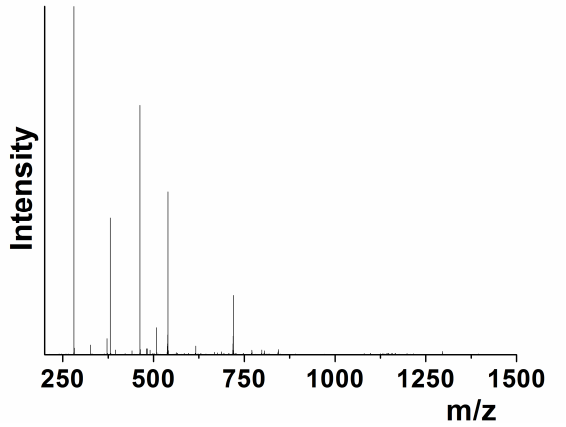

Figure S 6 Negative mode high resolution ESI mass spectrum of of compound **1**ca. 1 x 10^{-5} M in Methanol.

Table S 3 Peak assignments for ESI-MS Spectrum of compound **1** in MeOH.

recorded m/z	calculated m/z	peak assignment
280.79	280.79	$[V_3O_8]^{1-}$
380.72	380.73	$H[V_4O_{11}]^{1-}$ S4
462.65	462.65	$[V_{10}O_{26}]^{2-}$ S4
539.59[a]	539.60	$[BaV_{10}O_{27}]^{2-}$
616.55	616.55	$[Ba_2V_{10}O_{28}]^{2-}$
644.50	644.52	$[V_7O_{18}]^{1-}$
719.80	719.81	$H[Ba_2(V_{10}O_{27})_2]^{3-}$
771.10	771.11	$HBa_3[(V_{10}O_{27})(V_{10}O_{28})]^{3-}$
719.79	719.81	$HBa_2[(V_{10}O_{27})_2]^{3-}$
766.92	766.93	$Ba_2[(V_{10}O_{26})_2(V_{10}O_{27})]^{4-}$
805.39	805.41	$Ba_3[(V_{10}O_{26})(V_{10}O_{27})_2]^{4-}$
809.90	809.91	$H_2[Ba_3(V_{10}O_{27})_3]^{4-}$
814.41	814.41	$H_4[Ba_3(V_{10}O_{27})_2(V_{10}O_{28})]^{4-}$
843.87	843.88	$[Ba_4(V_{10}O_{27})_3]^{4-}$
848.38	848.38	$H_2[Ba_4(V_{10}O_{28})(V_{10}O_{27})_2]^{4-}$
852.88	852.89	$H_4[Ba_4(V_{10}O_{28})_2(V_{10}O_{27})]^{4-}$

891.14	891.15	$H[Ba_5(V_{10}O_{27})_4]^{5-}$
894.74	894.75	$H_3[Ba_5(V_{10}O_{27})_3(V_{10}O_{28})]^{5-}$
901.96	901.95	$H_7[Ba_5(V_{10}O_{28})_3(V_{10}O_{27})]^{5-}$
921.32	921.33	$H[Ba_6(V_{10}O_{28})(V_{10}O_{27})_3]^{5-}$
1086.20	1086.22	$[H_5Ba_3(V_{10}O_{27})_2(V_{10}O_{28})]^{3-}$
1098.20	1098.23	$H_6Ba_2[(V_{10}O_{28})_2]^{2-}$

4.3 CSI-MS (-35 ℃) measurements were performed on **compound** 1 (*ca*. 1 x 10^{-4} M in DMF/MeCN (1:4, v:v)) in negative (-ve) ion mode.

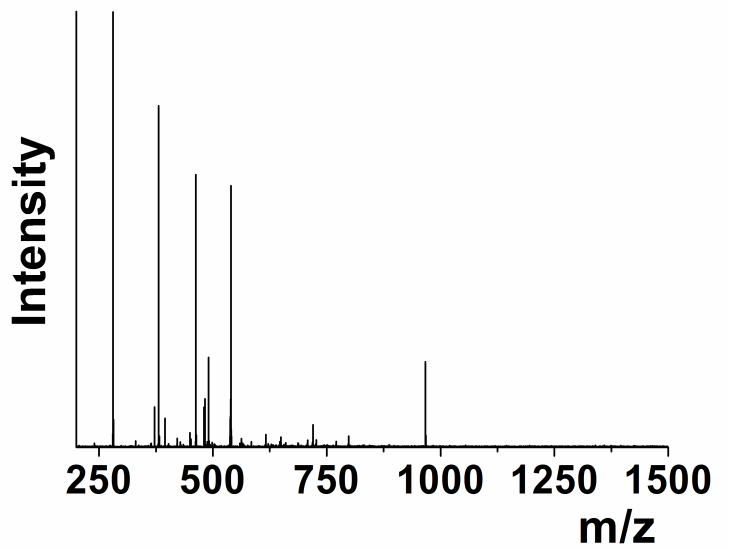

Figure S 7 Negative mode high resolution CSI mass spectrum of compound **1** ca. 1 x 10^{-4} M in DMF/MeCN (1:4, v:v).

Table S 4 Peak assignments for CSI-MS Spectrum of compound **1** in DMF/MeCN (1:4, v:v).

recorded m/z	**calculated m/z**	**peak assignment**
462.65	462.65	$[V_{10}O_{26}]^{2-}$ S4
480.66	480.6	$[V_{10}O_{28}]^{2-}$
539.59[a]	539.60	$[BaV_{10}O_{27}]^{2-}$
719.81	719.81	$H[Ba_2(V_{10}O_{27})_2]^{3-}$
725.81	725.81	$H_3Ba_2[(V_{10}O_{28})(V_{10}O_{27})]^{3-}$

731.81	731.81	$H_5Ba_2[(V_{10}O_{28})_2]^{3-}$
771.10	771.11	$HBa_3[(V_{10}O_{27})(V_{10}O_{28})]^{3-}$
719.79	719.81	$HBa_2[(V_{10}O_{27})_2]^{3-}$
805.41	805.41	$Ba_3[(V_{10}O_{26})(V_{10}O_{27})_2]^{4-}$
809.90	809.91	$H_2[Ba_3(V_{10}O_{27})_3]^{4-}$
814,41	814,41	$H_4[Ba_3(V_{10}O_{27})_2(V_{10}O_{28})]^{4-}$
818.91	818.92	$H_6[Ba_3(V_{10}O_{28})_2(V_{10}O_{27})]^{4-}$
823.42	823.42	$H_8[Ba_3(V_{10}O_{28})_3]^{4-}$
878.38	878.38	$H_{11}[Ba_4(V_{10}O_{28})_4]^{5-}$
1098.23	1098.23	$H_6Ba_2[(V_{10}O_{28})_2]^{2-}$

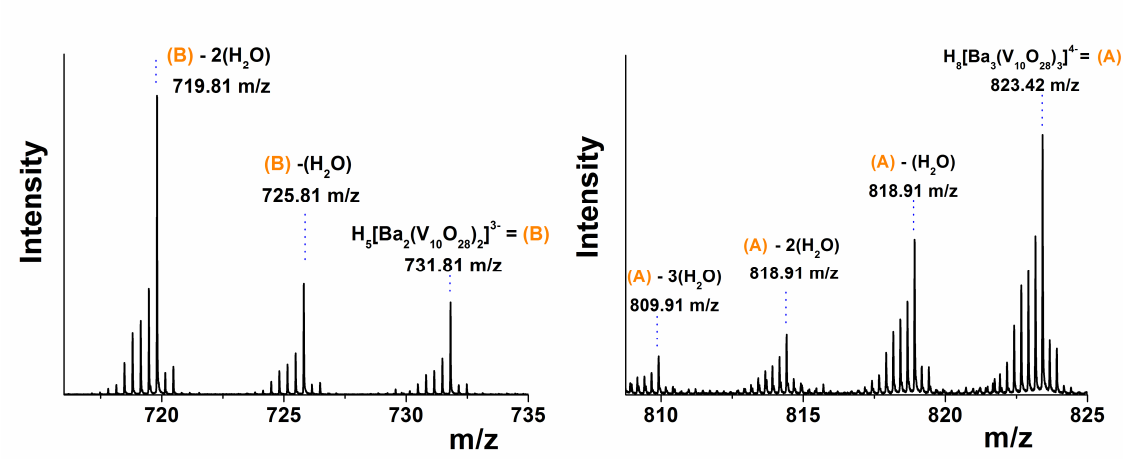

Figure S 8 Left: Peak assignment for the threefold negatively charged series of $H_5[Ba_2(V_{10}O_{28})_2]^{3-}$ (=(B)) and its fragment series with formal loss of one and two water molecules, respectively (mass region of m/z = *ca.* 721-734). Right: Peak assignment for the fourfold negatively charged series of $H_8[Ba_3(V_{10}O_{28})_3]^{4-}$ (=(A)) and its derivatives under the formal loss of one, two and three water molecules, respectively (mass region of m/z = *ca.* 809-825).

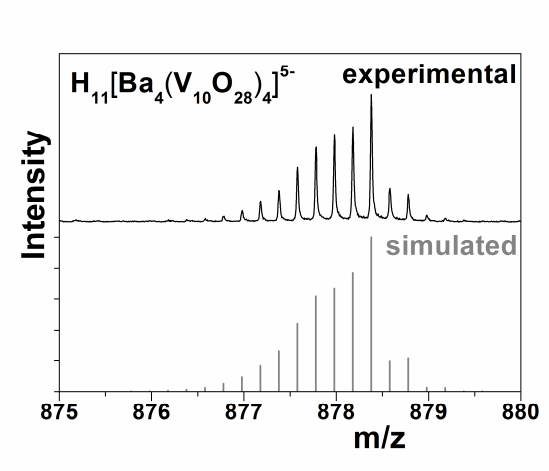

Figure S 9 Comparison of the experimental and simulated signals for the largest Ba-devanadate fragment assigned. It is formally assigned to $H_{11}[Ba_4(V_{10}O_{28})_4]^{5-}$ at m/z = 878.38.

4.4 CSI-MS (-35 ℃) measurements were performed on compound **2** (*ca*. 1 x 10^{-4} M in DMF/MeCN (1:4, v:v)) in negative (-ve) ion mode.

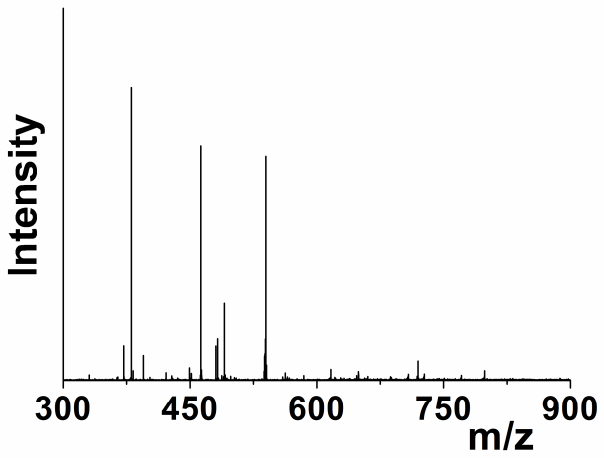

Figure S 10 Negative mode high resolution CSI mass spectrum of compound **2** ca. 1 x 10^{-4} M in DMF/MeCN (1:4, v:v).

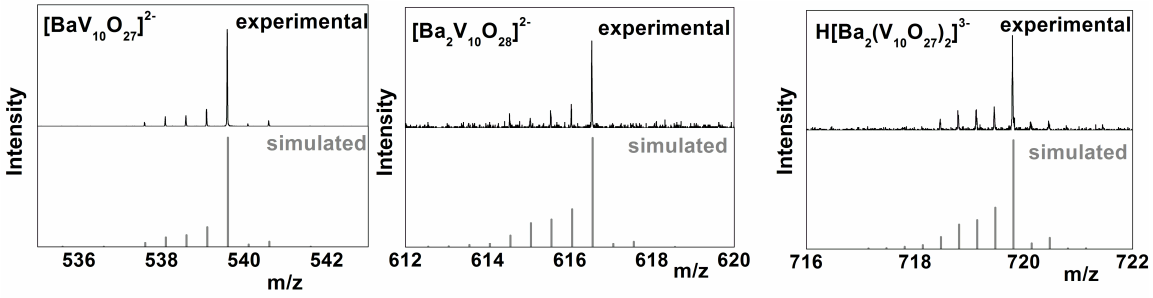

Figure S 11 Comparison of the experimental and simulated signals for the largest Ba-devanadate fragment, which could be detected via CSI-MS. The peak at m/z = 539.60 was assigned to $[Ba(V_{10}O_{27})]^{2-}$, the peak at m/z = 616.55 was assigned to at $[Ba_2(V_{10}O_{28})]^{2-}$, the peak at m/z = 719.81 was assigned to at H $[Ba_2(V_{10}O_{27})_2]^{3-}$.

Table S 5 Peak assignments for CSI-MS Spectrum of compound **2** ca. 1 x 10^{-4} M in DMF/MeCN (1:4, v:v).

recorded m/z	calculated m/z	peak assignment
280.79	280.79	$[V_6O_{16}]^{2-\ S4}$
462.65	462.65	$[V_{10}O_{26}]^{2-\ S4}$
380.72	380.72	$H[V_4O_{11}]^{1-\ S4}$
480.66	480.66	$H_4[V_{10}O_{28}]^{2-}$
539.60	539.60	$[BaV_{10}O_{27}]^{2-}$
616.55	616.55	$[Ba_2V_{10}O_{28}]^{2-}$
719.81	719.81	$H[Ba_2(V_{10}O_{27})_2]^{3-}$

5. Thermogravimetric analysis

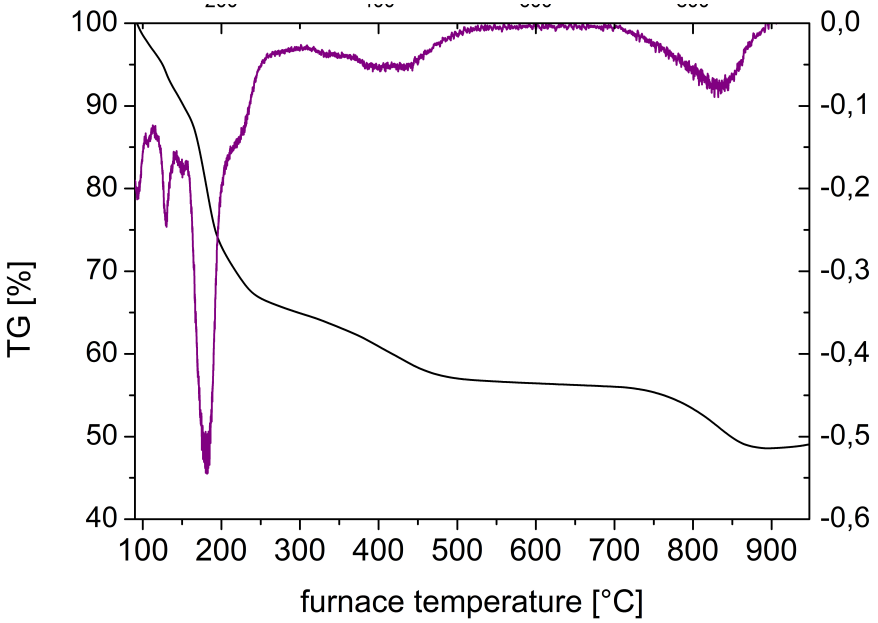

Figure S 12 Thermogravimetric analysis of compound **1**, indicating a first weight loss step (25 – 307.7 ℃) corresponding to eight water molecules an d 20 NMP molecules (11 solvent molecules and 9 ligand molecules) (observed: 35.31 wt.-%; calc: 35.20 wt.-%); the second weight loss step (307.7 – 574.5 ºC) corresponds to the loss of five ligand NMP molecules (observed: 8.14 wt.-%, calc: 8.20 wt.-%). Above 700 ℃ the cluster anion d ecomposes and the third weight loss step can be assigned to three $Ba(OH)_2$ molecules (white precipitate observed at the exhaust of the TGA instrument), whereby the protons from the cluster might serve as the proton source (observed: 7.96 wt.-%; calc: 8.49 wt.-%).

6. Literature references cited in Supporting Information

S1 G. M. Sheldrick, *Acta Crystallogr*., **2008**, *A64*, 112.

S2 L. J. Farrugia*, J. Appl. Cryst*., **1999**, *32*, 837.

S3 R. H. Blessing, *Acta Crystallogr. A,* **1995**, *51*, 33.

S4 T. Glone, J. Thiel, C. Streb, D.-L. Long, L. Cronin, *Chem. Commun*., **2012**, *48*, 359.